

University of Groningen

Magnetic and structural properties of Co nanocluster thin films

Koch, SA; Palasantzas, G; Vystavel, T; De Hosson, JTM; Binns, C; Louch, S

Published in:
Physical Review. B: Condensed Matter and Materials Physics

DOI:
[10.1103/PhysRevB.71.085410](https://doi.org/10.1103/PhysRevB.71.085410)

IMPORTANT NOTE: You are advised to consult the publisher's version (publisher's PDF) if you wish to cite from it. Please check the document version below.

Document Version
Publisher's PDF, also known as Version of record

Publication date:
2005

[Link to publication in University of Groningen/UMCG research database](#)

Citation for published version (APA):

Koch, SA., Palasantzas, G., Vystavel, T., De Hosson, JTM., Binns, C., & Louch, S. (2005). Magnetic and structural properties of Co nanocluster thin films. *Physical Review. B: Condensed Matter and Materials Physics*, 71(8), art. - 085410. [085410]. <https://doi.org/10.1103/PhysRevB.71.085410>

Copyright

Other than for strictly personal use, it is not permitted to download or to forward/distribute the text or part of it without the consent of the author(s) and/or copyright holder(s), unless the work is under an open content license (like Creative Commons).

The publication may also be distributed here under the terms of Article 25fa of the Dutch Copyright Act, indicated by the "Taverne" license. More information can be found on the University of Groningen website: <https://www.rug.nl/library/open-access/self-archiving-pure/taverne-amendment>.

Take-down policy

If you believe that this document breaches copyright please contact us providing details, and we will remove access to the work immediately and investigate your claim.

Downloaded from the University of Groningen/UMCG research database (Pure): <http://www.rug.nl/research/portal>. For technical reasons the number of authors shown on this cover page is limited to 10 maximum.

Magnetic and structural properties of Co nanocluster thin films

S. A. Koch, G. Palasantzas,* T. Vystavel, and J. Th. M. De Hosson

Department of Applied Physics, Materials Science Center and Netherlands Institute for Metals Research, University of Groningen, 9747 AG Groningen, The Netherlands

C. Binns and S. Louch

Department of Physics and Astronomy, University of Leicester, Leicester LE1 7RH, United Kingdom

(Received 3 September 2004; published 11 February 2005)

In this work we report on the magnetic characterization of thin films composed of gas-phase cobalt nanoclusters deposited on surfaces. Measurements of magnetization curves at ambient temperature indicate a strong exchange interaction between the clusters, while at cryogenic temperatures an exchange bias field appears. The latter confirms the existence of a ferromagnetic/antiferromagnetic core-shell system. Temperature-dependent magnetization measurements under zero-field-cooled conditions showed a rather broad maximum situated around 200 K. Magnetic force microscopy indicates the formation of a correlated super-spin-glass (CSSG) resulting from the frustration between the interparticle exchange interaction and the randomly oriented intraparticle anisotropy. The approach to saturation of the magnetization curves at 295 K is consistent with a CSSG.

DOI: 10.1103/PhysRevB.71.085410

PACS number(s): 68.37.Rt, 36.40.Cg, 61.46.+w, 68.37.Ps

I. INTRODUCTION

In a material composed of magnetic nanosized particles, the overall magnetic behavior is a result of both the properties of individual constituents and the interactions between them. Intrinsic particle properties¹ are determined by particle size, shape, structure, and composition. Magnetic anisotropy generates magnetic easy axes, with an energy barrier separating different orientations of the magnetic moment. In the absence of an external field the moment is in a blocked or frozen state, unless thermal activation is able to overcome the anisotropy energy barrier and induce flipping of the moment between easy directions (superparamagnetism). For a sufficiently low concentration of nanosized particles, the weak interparticle interactions can be incorporated in the effective energy barrier separating single-particle magnetization states. With increasing particle concentration, however, the interactions can eventually lead to spin glass behavior:² the assembly becomes a collection of magnetic moments having a disordered ground state with multiple stable configurations, rather than the uniform or periodic ground state arrangement in conventional magnets.

Typical spin glass phenomena, such as the presence of short-range spatial correlations and field-cooled/zero-field-cooled hysteresis, appear primarily at high particle concentrations and low temperatures.^{3,4} The transition from single-particle behavior to collective behavior is an important subject of study. In the latter situation, exchange coupling between randomly oriented nanosized grains often yields soft magnetic behavior,^{5,6} which is useful in technological applications such as power transformers, inductors, and high-frequency field-amplifying components (e.g., in read-write heads for computer disk memories). On the other hand, interparticle coupling may adversely affect the independence of individual nanometric storage units in magnetic recording media.

Unlike conventional spin glasses, which are dispersions of magnetic atoms in a nonmagnetic matrix, assemblies of mag-

netic nanosized particles possess internal dynamics. Notably, exposure of cobalt particles to oxygen induces an increase in magnetic anisotropy, resulting from the formation of an antiferromagnetic (AF) oxide phase around the ferromagnetic (FM) particle cores.⁷⁻¹⁰ When such a material is cooled in a strong field, the moments of the Co cores are oriented along the cooling field direction and blocked at low temperatures. Exchange coupling across the AF/FM interface polarizes AF spins close to the interface, forming an AF configuration that persists after the sample is cooled through the corresponding Néel temperature. The pinned AF domains produce an extra field acting on the particle core moments, leading to a shift of the hysteresis loop in a direction opposite to the cooling field.⁷⁻¹⁰ The shift is referred to as an exchange bias field (H_{eb}) and is the typical manifestation of unidirectional exchange anisotropy (UEA). It is a well-established experimental fact that exchange bias is accompanied by an enhancement of the coercivity H_c under field cooled conditions,⁷⁻¹⁰ although this effect is less well understood from a theoretical viewpoint. UEA exists up to a temperature T_g in the range of 150–200 K,⁷⁻¹⁰ which is well below the Néel temperature of bulk CoO ($T_N=293$ K). It is assumed that only below T_g is the interfacial AF spin configuration frozen and thus contributes to UEA.⁷ For Co/CoO particles of size $R=6$ nm, the field-cooled coercivity at 5 K was observed to be $H_c=0.3-0.4$ T and the exchange bias $H_{eb}=0.5$ T.⁷ Similar values were found for Co/CoO particles with a Co core of 3–4 nm and an oxide shell of 1 nm within a superparamagnetic matrix ($H_c=0.59$ T in the field-cooled case and $H_{eb}=0.92$ T).⁸

The extent of the ferromagnetic order due to interparticle interaction and its relation to the Co/CoO interface have not yet been investigated thoroughly from room temperature down to a few kelvin by combined magnetic and microscopy techniques. This will be the topic of the present work where magnetic force microscopy (MFM), hysteresis loop measurements, and high-resolution transmission electron microscopy

are combined to explore structural and magnetic properties of densely assembled Co nanosized cluster thin films.

II. EXPERIMENTAL PROCEDURE

Clusters of Co were produced with a cluster deposition source¹¹ that employs the gas aggregation principle. A supersaturated metal vapor is generated by sputtering a Co target in an inert gas atmosphere (Ar, at a partial pressure of 0.6–0.7 mbar). The condensation chamber is water cooled and it is evacuated to 1×10^{-7} mbar prior to the experiment. With a sputtering power of ~ 80 W and an aggregation length of 150 mm, clusters of size ~ 8 nm were obtained. Random stacking of these clusters on a substrate leads to the formation of a porous film, where the clusters remain largely intact due to their low impact energy.¹²

Samples for *ex situ* magnetometry measurements were deposited on polyetheretherketone (PEEK), a material with a very low diamagnetic response. After capping with a protective layer of Ag, analysis took place in an Oxford Instruments vibrating sample magnetometer (VSM). Magnetic hysteresis curves were measured both at 295 K, and at 2 K after field cooling with an applied field of 2 T. Furthermore, temperature-dependent magnetization of the cluster films was measured using a Quantum Design MPMS superconducting quantum interference device system in the temperature range from 4.2 to 300 K with an applied magnetic field of 1 T. In this case a substrate of *p*-type Si(100) was used, with a resistivity of 0.01 Ω cm and a negligible concentration of transition metal atoms.

High-resolution microscopy imaging and electron diffraction analysis were performed with a JEOL 2010F transmission electron microscope (TEM), on clusters supported on 25-nm-thick silicon nitride films or carbon-coated Formvar films (10 nm) attached to Cu specimen grids. Finally, magnetic stray fields from the Co cluster films supported on Si(100) substrates were imaged using magnetic force microscopy. Details of the MFM measurement procedure have been described previously.¹³

III. RESULTS AND DISCUSSION

Figure 1(a) shows a TEM image of a typical isolated Co cluster supported on a carbon-coated microscopy grid. The various projected external shapes that were observed correspond well with an icosahedral habit. Here the icosahedron is viewed along its twofold symmetry axis, while other clusters were observed to be in the “threefold” or “fivefold” orientations. Electron diffraction measurements [Fig. 1(b)] indicate a predominant fcc crystal phase in these samples, including only a small amount of hcp phase. The fraction of Co bulk phase (hcp) is known to increase with increasing cluster size.¹⁴

In addition, fcc cobalt oxide (CoO) was detected. Oxide peaks were more pronounced in some samples than in others, due to different times of exposure to air (the TEM samples were transferred into the electron microscope without a protective capping layer). In ambient air, Co clusters in this size range have been known to form an oxide shell of about 1 nm

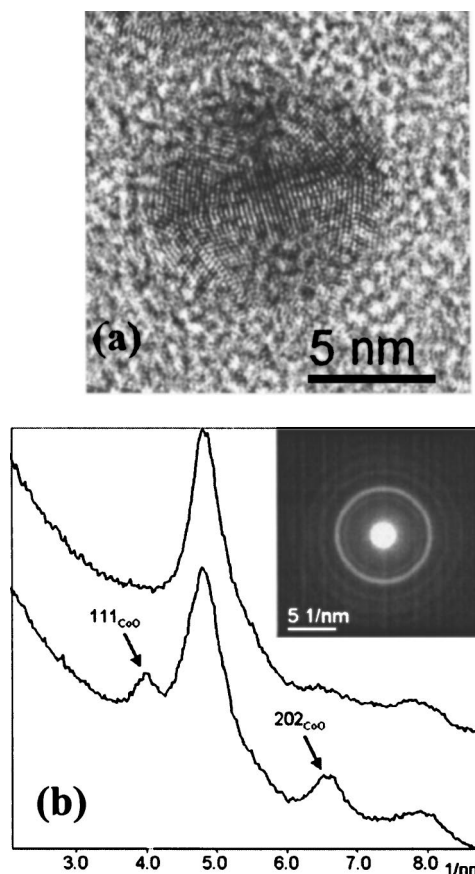


FIG. 1. (a) TEM image of an icosahedral Co cluster viewed along the twofold axis. (b) Electron diffraction ring pattern (inset for oxidized Co clusters) and integrated intensity of diffraction rings in the range 2.5–9 nm^{-1} (plot), for two Co cluster layers with different levels of oxidation. Arrows indicate peaks arising from CoO with the corresponding Miller indices for the oxide. Spacing of diffraction spots in reciprocal space is measured in units of nm^{-1} .

thickness, while smaller (~ 2 nm) clusters are completely converted into oxide.¹⁰ Our TEM images [Fig. 1(a)] suggest that the shell thickness is less than 1 nm, contrary to the earlier case of Fe clusters where it was significantly larger (~ 2 nm).¹⁵ The magnetometry samples were capped with a protective Ag layer prior to removal from the deposition chamber, but the exchange bias observed in the low-temperature magnetometry data shows that these clusters also had a CoO shell. At present it is not clear whether the oxide shell formed within the deposition source or through imperfections in the capping layer but as we argue below, it is clear that most of the clusters are core-shell systems.

A magnetization curve obtained from a continuous cluster film at 295 K in the VSM is displayed in Fig. 2(a). The data are averaged from three separate scans with a negative field sweep (down) and three separate scans with a positive field sweep (up), while the diamagnetic contribution from the sample holder has been subtracted. The Co cluster film on PEEK has a soft magnetization curve, as expected for a strongly interacting assembly. After cooling in a field of 2 T to a temperature of 2 K, hysteresis curves were measured according to the same procedure. In this case the loop is

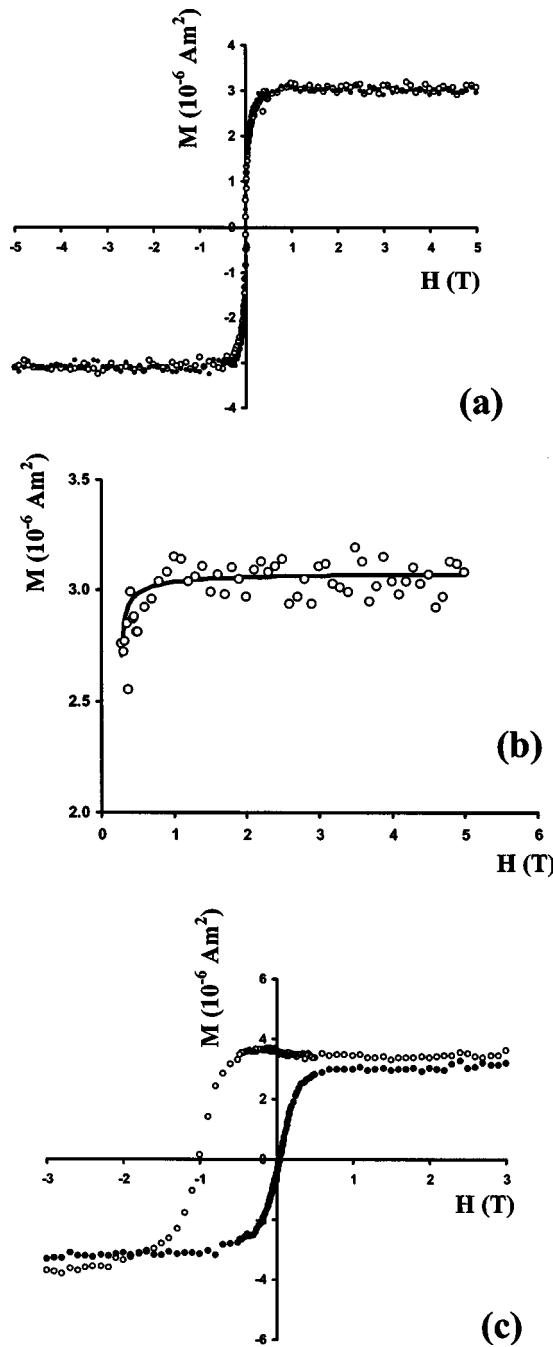


FIG. 2. Magnetic hysteresis loops at (a) 295 and (c) 2 K. The loop shift for the latter is about 0.5 T. (b) is a detail of (a) showing the predicted approach to saturation for a CSSG with $\lambda_r=0.67$ (line).

shifted from zero, and a large coercive field H_c appears [Fig. 2(b)]. The unidirectional loop shift reflects the presence of an antiferromagnetic oxide coating on the clusters as discussed above. An important feature of the data is the uniform exchange bias over the whole range indicating that most of the clusters have a (partial or complete) oxide shell. In a system with a mixture of pure Co and Co/CoO core-shell clusters the magnetization shows a mixture of shifted and unshifted loops.¹⁶ Apart from an exchange bias field $H_{eb} \sim 0.5$ T, a coercive field $H_c \sim 0.5$ T was found. Enhancement of coer-

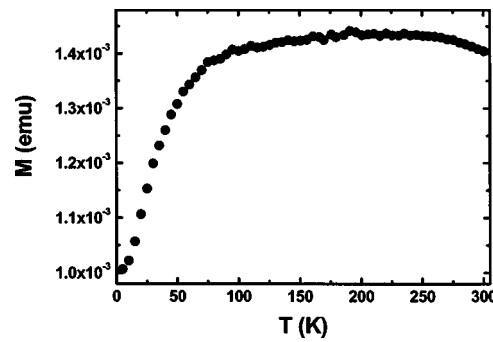


FIG. 3. Zero-field-cooled magnetization measured as a function of temperature under an applied field of 1 T. The arrow indicates the approximate position of the maximum.

civity is another critical characteristic of exchange bias systems.

The large bias fields observed may suggest the existence of antiferromagnetic noncollinear moment configurations that are found in magnetic oxide nanoparticles.¹⁰ This is consistent with earlier studies where a spin disorder at the Co/CoO interface was invoked to explain the induced uniaxial anisotropy $K_{ux} \approx H_c M_s$.⁷ If we compare with the unidirectional exchange anisotropy $K_{uae} \approx H_{eb} M_s$, then we obtain $K_{ux}/K_{uae} \approx H_c/H_{eb} \approx 1$. Therefore, the ferromagnetic-antiferromagnetic interface coupling leads to the formation of a large uniaxial anisotropy due to the particle exchange interaction. The ultrathin oxide shell (<1 nm) will not produce exchange bias in isolated Co particles,¹⁰ but for dense assemblies the effect is readily observed. This behavior shows that interparticle coupling stabilizes the ferromagnetism of the particle core as well as the antiferromagnetism of the particle shell.¹⁰

For zero-field-cooled magnetization measurements, a 375-nm-thick Co cluster film was cooled to 4.2 K in the absence of an applied field and magnetization was measured as the sample was heated to 300 K. As shown in Fig. 3, the magnetization increases monotonically as thermal vibration provides the activation energy to align an increasing number of moments with the external field. The approach to saturation is rather fast, and the maximum where the highest number of moments are aligned with the external field is situated around 200 K (which is close to the temperature T_g where the interfacial AF spin configuration is frozen) in agreement with former studies.⁷⁻¹⁰ The peak is, however, very broad and no single superparamagnetic blocking temperature can be identified from these data. As ambient temperature is approached, thermal vibrations become strong enough to randomize some of the moments once again, leading to the observed slight decrease in magnetization. The temperature at which the blocking transition occurs primarily depends on particle volume, and a broad maximum such as this may result from a wide distribution of particle sizes. However, TEM observations of isolated Co clusters have indicated that the statistical variation in particle diameter is only about 10% for these samples. It is possible that the level of oxidation is not uniformly distributed over the clusters. The transition temperature is influenced by the extent to which the core magnetization is pinned by its antiferromagnetic shell,⁸ and

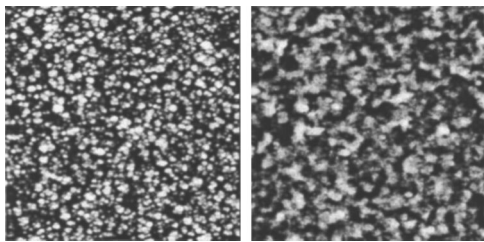


FIG. 4. Topography and phase images of a closed film (of thickness 375 nm) with scan size 5000 nm.

therefore such inhomogeneities might lead to the observed temperature distribution.

Although at room temperature the presence of an oxide shell ceases to have any effect, magnetic force microscopy has provided further evidence of exchange coupling between the Co grains.¹³ Figure 4 shows topography and MFM phase images obtained on a continuous Co nanocluster film under ambient conditions. The phase data show magnetic correlations that clearly extend beyond the size of a single cluster. In fact, we have calculated from the MFM data a magnetic correlation length $\xi \approx 200$ nm, compared to a topographic correlation length close to 90 nm.¹³ The existence of magnetic correlations can be interpreted in the context of the random anisotropy model developed^{17–19} and previously applied to Fe and Co cluster films.^{6,20,21} In this formalism two competing terms are defined as the random anisotropy field H_r , and the interparticle exchange field H_{ex} :

$$H_r = 2K_r/M_s, \quad H_{ex} = 2A/M_s R_a^2, \quad (1)$$

where R_a is the nanometer-sized region over which the local anisotropy axis is correlated (i.e., the cluster size), A and K_r the exchange and anisotropy constants, and M_s the saturation magnetization. Their relative strength determines the magnetic ground state and it is specified by the dimensionless parameter

$$\lambda_r = \frac{H_r}{H_{ex}} = \frac{K_r R_a^2}{A}. \quad (2)$$

In the case of high anisotropy and/or low exchange coupling ($\lambda_r > 1$), the magnetic vector in each particle points along the local intraparticle anisotropy axis. With decreasing λ_r the magnetization vectors in neighboring particles are increasingly aligned, but the stochastic perturbation produced by the random distribution of anisotropy axes results in a mesoscopic correlation length with no long-range order. This con-

figuration is known as a correlated super-spin-glass (CSSG).^{17–19} Indeed, a spin-glass state in general arises from a competition among the different interactions acting on the magnetic moments, and the random character of these interactions.² For the present system we find from the observed magnetic correlation length a ratio of $\lambda_r = 0.67$,¹³ indicating a rather strong exchange interaction which is consistent with the soft magnetic behavior at room temperature. Figure 2(b) shows the predicted approach to saturation for a CSSG with $\lambda_r = 0.67$ (line) and it is observed to fit the data well. There is too much scatter in the data to obtain an optimized fit as a function of the CSSG parameters but clearly the magnetization data are consistent with the CSSG state.

At lower temperatures the presence of the CoO will contribute to the uniaxial anisotropy, thus increasing the ratio λ_r and weakening the CSSG state. Note that as the maximum dipolar field between two nanosized particles in contact amounts to about 0.07 T,¹⁰ the interparticle dipolar interactions are not the source of the effects described here since for example the exchange interaction is of the order of 1 T.

IV. CONCLUSIONS

In summary, dense deposits of Co nanoclusters form a strongly interacting system as indicated by magnetization measurements and magnetic force microscopy. Exchange coupling between the particles results in soft magnetic behavior at room temperature. However, disorder is introduced by the random anisotropy directions so that correlated areas remain limited in size, in agreement with the correlated super-spin-glass configuration. At cryogenic temperatures an exchange bias field appears after field-cooling procedures, indicating unidirectional exchange coupling between ferromagnetic particle cores and antiferromagnetic oxide shells. Despite its small thickness (< 1 nm) the oxide phase is capable of producing a large exchange bias and coercivity. The values observed are in agreement with those of former studies that suggested the existence of antiferromagnetic noncollinear moment configurations at the AF/FM interfaces. The presence of interparticle interactions is shown to play a role in stabilizing both ferromagnetic and antiferromagnetic order in Co/O nanocluster assemblies.

ACKNOWLEDGMENT

We would like to acknowledge financial support from the Materials Science Center MSC^{plus} program at the University of Groningen.

*Corresponding author. Email address: g.palasantzas@phys.rug.nl

¹R. H. Kodama, *J. Magn. Magn. Mater.* **200**, 359 (1999).

²P. E. Jönsson, *Adv. Chem. Phys.* **128**, 191 (2004).

³W. Luo, S. R. Nagel, T. F. Rosenbaum, and R. E. Rosensweig, *Phys. Rev. Lett.* **67**, 2721 (1991).

⁴H. Mamiya, I. Nakatami, and T. Furubayashi, *Phys. Rev. Lett.* **82**, 4332 (1999).

⁵J. F. Löffler, H.-B. Braun, and W. Wagner, *Phys. Rev. Lett.* **85**, 1990 (2000).

⁶C. Binns, M. J. Maher, Q. A. Pankhurst, D. Kechrakos, and K. N. Trohidou, *Phys. Rev. B* **66**, 184413 (2002).

⁷D. L. Peng, K. Sumiyama, T. Hihara, S. Yamamuro, and T. J. Konno, *Phys. Rev. B* **61**, 3103 (2000).

⁸R. Morel, A. Brenac, and C. Portemont, *J. Appl. Phys.* **95**, 3757

- (2004).
- ⁹S. Gangopadhyay, G. C. Hadjipanayis, C. M. Sorensen, and K. J. Klabunde, *J. Appl. Phys.* **73**, 6964 (1993).
- ¹⁰V. Skumryev, S. Stoyanov, Y. Zhang, G. Hadjipanayis, D. Givord, and J. Nogues, *Nature (London)* **423**, 850 (2003).
- ¹¹For details on our deposition system see <http://www.oaresearch.co.uk/cluster.htm>
- ¹²H. Haberland, Z. Insepov, and M. Moseler, *Phys. Rev. B* **51**, 11 061 (1995); G. Palasantzas, S. A. Koch, and J. Th. M. De Hosson, *Rev. Adv. Mater. Sci.* **5**, 57 (2003).
- ¹³S. A. Koch, R. H. te Velde, G. Palasantzas, and J. Th. M. De Hosson, *Appl. Surf. Sci.* **226**, 185 (2004); *Appl. Phys. Lett.* **84**, 556 (2004).
- ¹⁴O. Kitakami, H. Sato, Y. Shimada, F. Sato, and M. Tanaka, *Phys. Rev. B* **56**, 13 849 (1997).
- ¹⁵T. Vystavel, G. Palasantzas, S. A. Koch, and J. Th. M. De Hosson, *Appl. Phys. Lett.* **82**, 197 (2003).
- ¹⁶J. M. Meldrim, Y. Qiang, Y. Liu, H. Haberland, and D. J. Sellmyer, *J. Appl. Phys.* **87**, 7013 (2000).
- ¹⁷E. M. Chudnovsky, *J. Magn. Magn. Mater.* **40**, 21 (1983).
- ¹⁸E. M. Chudnovsky, W. M. Saslow, and R. A. Serota, *Phys. Rev. B* **33**, 251 (1986).
- ¹⁹W. M. Saslow, *Phys. Rev. B* **35**, 3454 (1987).
- ²⁰C. Binns and M. J. Maher, *New J. Phys.* **1**, 1.1 (2002).
- ²¹J. F. Löffler, J. P. Meier, B. Doudin, J-P. Ansermet, and W. Wagner, *Phys. Rev. B* **57**, 2915 (1998).